

# Spectroscopy and Regge trajectories of heavy baryons in the relativistic quark-diquark picture

D. Ebert<sup>1</sup>, R. N. Faustov<sup>1,2</sup> and V. O. Galkin<sup>1,2</sup>

<sup>1</sup> *Institut für Physik, Humboldt-Universität zu Berlin,  
Newtonstr. 15, D-12489 Berlin, Germany*

<sup>2</sup> *Dorodnicyn Computing Centre, Russian Academy of Sciences,  
Vavilov Str. 40, 119991 Moscow, Russia*

Mass spectra of heavy baryons are calculated in the heavy-quark–light-diquark picture in the framework of the QCD-motivated relativistic quark model. The dynamics of light quarks in the diquark as well as the dynamics of the heavy quark and light diquark in the baryon are treated completely relativistically without application of nonrelativistic  $v/c$  and heavy quark  $1/m_Q$  expansions. Such approach allows us to get predictions for the heavy baryon masses for rather high orbital and radial excitations. On this basis the Regge trajectories of heavy baryons for orbital and radial excitations are constructed, and their linearity, parallelism, and equidistance are verified. The relations between the slopes and intercepts of heavy baryons are considered and a comparison of the slopes of Regge trajectories for heavy baryons and heavy-light mesons is performed. All available experimental data on heavy baryons fit nicely to the constructed Regge trajectories. The possible assignment of the quantum numbers to the observed excited charmed baryons is discussed.

PACS numbers: 14.20.Lq, 14.20.Mr, 12.39.Ki

## I. INTRODUCTION

Recently a significant experimental progress has been achieved in studying the heavy baryon spectroscopy. In the last five years the number of the observed charmed and bottom baryons almost doubled and now it is nearly the same as the number of known charmed and bottom mesons [1]. Observations of new charmed baryons were mainly done at the  $B$ -factories, while new bottom baryons were discovered at Tevatron [2]. It is expected that new data on excited bottom baryons will come soon from the LHC, where they are supposed to be copiously produced. Due to the poor statistics, the quantum numbers of most of the excited states of heavy baryons are not known experimentally and are usually prescribed following the quark model predictions [1].

In this paper we investigate heavy baryon spectroscopy in the framework of the QCD-motivated relativistic quark model based on the quasipotential approach [3, 4]. To simplify the very complicated relativistic three-body problem heavy baryons are considered in the heavy-quark–light-diquark approximation. This reduces the initial three-body problem to two step two-body calculations. First, the light diquark properties, such as masses and form factors, are presented [4]. Then a heavy baryon is considered as the bound system of a heavy quark and a light diquark. In order to take into account the rather large size

and structure of the light diquark, its nonlocal interaction with gluons is described by the form factor expressed in terms of the diquark wave functions. All heavy baryon excitations, both orbital and radial, are assumed to occur in the bound system of the heavy quark and light diquark, while the latter is taken only in the ground (scalar or axial vector) state. Such scheme significantly reduces the number of the excited baryon states compared to the genuine three-quark picture. The goal of this paper is the calculation of the masses of the excited heavy baryons up to rather high orbital and radial excitations. This will allow us to construct the heavy baryon Regge trajectories both in the  $(J, M^2)$  and  $(n_r, M^2)$  planes, where  $J$  is the baryon spin,  $M$  is the baryon mass and  $n_r$  is the radial quantum number. Then we can test their linearity, parallelism and equidistance and determine their parameters: Regge slopes and intercepts. Their determination is of great importance, since they provide a better understanding of the hadron dynamics. Moreover, their knowledge is also important for non-spectroscopic problems such as, e.g., hadron production and high energy scattering. Since we are going to calculate highly excited heavy baryon states it is important to use a fully relativistic approach, which does not use the nonrelativistic  $v/c$  expansion for light quarks and diquarks and does not employ the heavy quark  $1/m_Q$  expansion for the heavy quark.

The heavy baryon spectroscopy has been extensively studied in the literature [2, 4–13]. Various quark models [2, 4–8, 13], heavy quark  $1/m_Q$  and  $1/N_c$  expansions [9], quenched and unquenched lattice calculations [10, 11] and QCD sum rules [12] have been used. However, in all these calculations either masses of the ground state baryons were obtained or only a few lowest orbital and radial excitations were considered. Therefore the Regge trajectories of heavy baryons have not been constructed. Contrarily, the Regge trajectories of light baryons received significant attention [2, 14–21]. The related investigations were performed on the basis of quark models [14–17], empirical relations [19] and in models based on the AdS/QCD duality [20, 21]. It was shown that the highly orbitally excited light baryons have an antisymmetric structure of the quark-diquark type [14, 15] and such configuration minimizes the energy [14]. Only in this case light baryon and meson Regge trajectories have the same slope [14, 15]<sup>1</sup> which is in agreement with experimental data.

Several simple relations between slopes and intercepts of light and heavy baryons have been deduced in different models within QCD (see, e.g., [16, 22, 23] and references therein). They were used for obtaining various linear and quadratic mass relations between baryon masses [23].

The paper is organized as follows. In Sec. II we present the relativistic quark-diquark model of heavy baryons. First we discuss properties of light diquarks and give their masses and form factors. Then a heavy baryon is considered as the bound system of a heavy quark and a light diquark. The completely relativistic expressions for the corresponding quasipotentials are given. In Sec. III the heavy baryon spectroscopy is presented and discussed. Our predictions for charmed and bottom baryon masses are confronted with the available experimental data. The obtained results are used for constructing the heavy baryon Regge trajectories both in the  $(J, M^2)$  and  $(n_r, M^2)$  planes. The prescription of the observed baryon states to the particular trajectory allows to determine their quantum numbers. Then we obtain slopes and intercepts of parent and daughter trajectories and test the proposed relations between them. Finally, a comparison of the slopes of the heavy meson and heavy baryon Regge trajectories is performed. We present our conclusions in Sec. IV.

---

<sup>1</sup> Note that all these considerations were done for massless scalar quarks.

## II. RELATIVISTIC QUARK-DIQUARK MODEL OF HEAVY BARYONS

In the quasipotential approach and quark-diquark picture of heavy baryons the interaction of two light quarks in a diquark and the heavy quark interaction with a light diquark in a baryon are described by the diquark wave function ( $\Psi_d$ ) of the bound quark-quark state and by the baryon wave function ( $\Psi_B$ ) of the bound quark-diquark state respectively, which satisfy the quasipotential equation of the Schrödinger type [3]

$$\left( \frac{b^2(M)}{2\mu_R} - \frac{\mathbf{p}^2}{2\mu_R} \right) \Psi_{d,B}(\mathbf{p}) = \int \frac{d^3q}{(2\pi)^3} V(\mathbf{p}, \mathbf{q}; M) \Psi_{d,B}(\mathbf{q}), \quad (1)$$

where the relativistic reduced mass is

$$\mu_R = \frac{M^4 - (m_1^2 - m_2^2)^2}{4M^3}, \quad (2)$$

and  $E_1, E_2$  are given by

$$E_1 = \frac{M^2 - m_2^2 + m_1^2}{2M}, \quad E_2 = \frac{M^2 - m_1^2 + m_2^2}{2M}. \quad (3)$$

Here  $M = E_1 + E_2$  is the bound state mass (diquark or baryon),  $m_{1,2}$  are the masses of light quarks ( $q_1$  and  $q_2$ ) which form the diquark or of the light diquark ( $d$ ) and heavy quark ( $Q$ ) which form the heavy baryon ( $B$ ), and  $\mathbf{p}$  is their relative momentum. In the center of mass system the relative momentum squared on mass shell reads

$$b^2(M) = \frac{[M^2 - (m_1 + m_2)^2][M^2 - (m_1 - m_2)^2]}{4M^2}. \quad (4)$$

The kernel  $V(\mathbf{p}, \mathbf{q}; M)$  in Eq. (1) is the quasipotential operator of the quark-quark or quark-diquark interaction. It is constructed with the help of the off-mass-shell scattering amplitude, projected onto the positive energy states. In the following analysis we closely follow the similar construction of the quark-antiquark interaction in mesons which were extensively studied in our relativistic quark model [3]. For the quark-quark interaction in a diquark we use the relation  $V_{qq} = V_{q\bar{q}}/2$  arising under the assumption about the octet structure of the interaction from the difference of the  $qq$  and  $q\bar{q}$  colour antitriplet and singlet states. An important role in this construction is played by the Lorentz-structure of the nonperturbative confining interaction. In our analysis of mesons, while constructing the quasipotential of the quark-antiquark interaction, we adopted that the effective interaction is the sum of the usual one-gluon exchange term with the mixture of long-range vector and scalar linear confining potentials, where the vector confining potential contains the Pauli term. We use the same conventions for the construction of the quark-quark and quark-diquark interactions in the baryon. The quasipotential is then defined by the following expressions [3, 24]

(a) for the quark-quark ( $qq$ ) interaction in the colour antitriplet state

$$V(\mathbf{p}, \mathbf{q}; M) = \bar{u}_1(p)\bar{u}_2(-p)\mathcal{V}(\mathbf{p}, \mathbf{q}; M)u_1(q)u_2(-q), \quad (5)$$

with

$$\mathcal{V}(\mathbf{p}, \mathbf{q}; M) = \frac{1}{2} \left[ \frac{4}{3} \alpha_s D_{\mu\nu}(\mathbf{k}) \gamma_1^\mu \gamma_2^\nu + V_{\text{conf}}^V(\mathbf{k}) \Gamma_1^\mu(\mathbf{k}) \Gamma_{2;\mu}(-\mathbf{k}) + V_{\text{conf}}^S(\mathbf{k}) \right],$$

(b) for quark-diquark ( $Qd$ ) interaction in the colour singlet state

$$\begin{aligned}
V(\mathbf{p}, \mathbf{q}; M) = & \frac{\langle d(P)|J_\mu|d(Q)\rangle}{2\sqrt{E_d(p)E_d(q)}} \bar{u}_Q(p) \frac{4}{3} \alpha_s D_{\mu\nu}(\mathbf{k}) \gamma^\nu u_Q(q) \\
& + \psi_d^*(P) \bar{u}_Q(p) J_{d;\mu} \Gamma_Q^\mu(\mathbf{k}) V_{\text{conf}}^V(\mathbf{k}) u_Q(q) \psi_d(Q) \\
& + \psi_d^*(P) \bar{u}_Q(p) V_{\text{conf}}^S(\mathbf{k}) u_Q(q) \psi_d(Q),
\end{aligned} \tag{6}$$

where  $\alpha_s$  is the QCD coupling constant,  $\langle d(P)|J_\mu|d(Q)\rangle$  is the vertex of the diquark-gluon interaction which takes into account the diquark internal structure,  $P = (E_d(p), -\mathbf{p})$ ,  $Q = (E_d(q), -\mathbf{q})$  and  $E_d(p) = \sqrt{\mathbf{p}^2 + M_d^2}$ .  $D_{\mu\nu}$  is the gluon propagator in the Coulomb gauge,  $\mathbf{k} = \mathbf{p} - \mathbf{q}$ ;  $\gamma_\mu$  and  $u(p)$  are the Dirac matrices and spinors

$$u^\lambda(p) = \sqrt{\frac{\epsilon(p) + m}{2\epsilon(p)}} \begin{pmatrix} 1 \\ \frac{\boldsymbol{\sigma}\mathbf{p}}{\epsilon(p) + m} \end{pmatrix} \chi^\lambda, \tag{7}$$

with  $\epsilon(p) = \sqrt{\mathbf{p}^2 + m^2}$ .

The diquark state in the confining part of the quark-diquark quasipotential (6) is described by the wave functions

$$\psi_d(p) = \begin{cases} 1 & \text{for the scalar diquark} \\ \varepsilon_d(p) & \text{for the axial vector diquark} \end{cases}, \tag{8}$$

where  $\varepsilon_d$  is the polarization vector of the axial vector diquark. The effective long-range vector vertex of the diquark can be presented in the form

$$J_{d;\mu} = \begin{cases} \frac{(P+Q)_\mu}{2\sqrt{E_d(p)E_d(q)}} & \text{for the scalar diquark} \\ -\frac{(P+Q)_\mu}{2\sqrt{E_d(p)E_d(q)}} + \frac{i\mu_d}{2M_d} \Sigma_\mu^\nu \tilde{k}_\nu & \text{for the axial vector diquark} \end{cases}, \tag{9}$$

where  $\tilde{k} = (0, \mathbf{k})$ . Here  $\Sigma_\mu^\nu$  is the antisymmetric tensor

$$(\Sigma_{\rho\sigma})_\mu^\nu = -i(g_{\mu\rho}\delta_\sigma^\nu - g_{\mu\sigma}\delta_\rho^\nu), \tag{10}$$

and the axial vector diquark spin  $\mathbf{S}_d$  is given by  $(S_{d;k})_{il} = -i\varepsilon_{kil}$ . We choose the total chromomagnetic moment of the axial vector diquark  $\mu_d = 0$  [25].

The effective long-range vector vertex of the quark is defined by [3, 26]

$$\Gamma_\mu(\mathbf{k}) = \gamma_\mu + \frac{i\kappa}{2m} \sigma_{\mu\nu} \tilde{k}^\nu, \quad \tilde{k} = (0, \mathbf{k}), \tag{11}$$

where  $\kappa$  is the Pauli interaction constant characterizing the anomalous chromomagnetic moment of quarks. In the configuration space the vector and scalar confining potentials in the nonrelativistic limit reduce to

$$\begin{aligned}
V_{\text{conf}}^V(r) &= (1 - \varepsilon)V_{\text{conf}}(r), \\
V_{\text{conf}}^S(r) &= \varepsilon V_{\text{conf}}(r),
\end{aligned} \tag{12}$$

with

$$V_{\text{conf}}(r) = V_{\text{conf}}^S(r) + V_{\text{conf}}^V(r) = Ar + B, \quad (13)$$

where  $\varepsilon$  is the mixing coefficient.

The constituent quark masses  $m_u = m_d = 0.33$  GeV,  $m_s = 0.5$  GeV,  $m_c = 1.55$  GeV,  $m_b = 4.88$  GeV, and the parameters of the linear potential  $A = 0.18$  GeV<sup>2</sup> and  $B = -0.3$  GeV have the usual values of quark models. The value of the mixing coefficient of vector and scalar confining potentials  $\varepsilon = -1$  has been determined from the consideration of charmonium radiative decays [27] and the heavy quark expansion [28]. Finally, the universal Pauli interaction constant  $\kappa = -1$  has been fixed from the analysis of the fine splitting of heavy quarkonia  $^3P_J$ - states [27]. Note that the long-range chromomagnetic contribution to the potential in our model is proportional to  $(1 + \kappa)$  and thus vanishes for the chosen value of  $\kappa = -1$ .

Since we deal with diquarks and baryons containing light quarks we adopt for the QCD coupling constant  $\alpha_s(\mu^2)$  the simplest model with freezing [29], namely

$$\alpha_s(\mu^2) = \frac{4\pi}{\beta_0 \ln \frac{\mu^2 + M_B^2}{\Lambda^2}}, \quad \beta_0 = 11 - \frac{2}{3}n_f, \quad (14)$$

where the scale is taken as  $\mu = 2m_1m_2/(m_1 + m_2)$ , the background mass is  $M_B = 2.24\sqrt{A} = 0.95$  GeV [29], and  $\Lambda = 413$  MeV was fixed from fitting the  $\rho$  mass [31]. Note that an other popular parametrization of  $\alpha_s$  with freezing [30] leads to close values.

### A. Light diquarks

At the first step, we present the masses and form factors of the light diquark [4]. As it is well known, the light quarks are highly relativistic, which makes the  $v/c$  expansion inapplicable and thus, a completely relativistic treatment is required. To achieve this goal in describing light diquarks, we closely follow our consideration of the light meson spectra [32] and adopt the same procedure to make the relativistic quark potential local by replacing  $\varepsilon_{1,2}(p) = \sqrt{m_{1,2}^2 + \mathbf{p}^2} \rightarrow E_{1,2}$  (see (3) and discussion in Ref. [32]).

The quasipotential equation (1) is solved numerically for the complete relativistic potential which depends on the diquark mass in a complicated highly nonlinear way [4]. The obtained ground state masses of scalar and axial vector light diquarks are presented in Table I.

In order to determine the diquark interaction with the gluon field  $\langle d(P)|J_\mu|d(Q)\rangle$ , which takes into account the diquark structure, it is necessary to calculate the corresponding matrix element of the quark current between diquark states. This diagonal matrix element can be parametrized by the set of elastic form factors in the following way

(a) scalar diquark ( $d = S$ )

$$\langle S(P)|J_\mu|S(Q)\rangle = h_+(k^2)(P + Q)_\mu, \quad (15)$$

(b) axial vector diquark ( $d = A$ )

$$\begin{aligned} \langle A(P)|J_\mu|A(Q)\rangle = & -[\varepsilon_d^*(P) \cdot \varepsilon_d(Q)]h_1(k^2)(P + Q)_\mu \\ & + h_2(k^2) \left\{ [\varepsilon_d^*(P) \cdot Q]\varepsilon_{d;\mu}(Q) + [\varepsilon_d(Q) \cdot P]\varepsilon_{d;\mu}^*(P) \right\} \end{aligned}$$

TABLE I: Masses  $M$  and form factor parameters of diquarks.  $S$  and  $A$  denote scalar and axial vector diquarks which are antisymmetric  $[\cdot\cdot\cdot]$  and symmetric  $\{\cdot\cdot\cdot\}$  in flavour, respectively [4].

Quark content	Diquark type	$M$ (MeV)	$\xi$ (GeV)	$\zeta$ (GeV <sup>2</sup> )
$[u, d]$	S	710	1.09	0.185
$\{u, d\}$	A	909	1.185	0.365
$[u, s]$	S	948	1.23	0.225
$\{u, s\}$	A	1069	1.15	0.325
$\{s, s\}$	A	1203	1.13	0.280

$$+h_3(k^2)\frac{1}{M_A^2}[\varepsilon_d^*(P)\cdot Q][\varepsilon_d(Q)\cdot P](P+Q)_\mu, \quad (16)$$

where  $k = P - Q$  and  $\varepsilon_d(P)$  is the polarization vector of the axial vector diquark.

The calculation of the matrix element of the quark current  $J_\mu = \bar{q}\gamma^\mu q$  between the diquark states leads to the emergence of the form factor  $F(r)$  entering the vertex of the diquark-gluon interaction [4]. Then the elastic form factors in Eqs. (15) and (16) are expressed by

$$\begin{aligned} h_+(k^2) &= h_1(k^2) = h_2(k^2) = F(\mathbf{k}^2), \\ h_3(k^2) &= 0, \end{aligned}$$

where the form factor  $F(r)$  is given by the overlap integral of the diquark wave functions. Using the numerical diquark wave functions we find that  $F(r)$  can be approximated with high accuracy by the expression [4]

$$F(r) = 1 - e^{-\xi r - \zeta r^2}. \quad (17)$$

The values of the parameters  $\xi$  and  $\zeta$  for the ground states of the scalar  $[q, q']$  and axial vector  $\{q, q'\}$  light diquarks are given in Table I.

## B. Heavy baryons as heavy-quark–light-diquark bound systems

At the second step, we calculate the masses of heavy baryons as the bound states of a heavy quark and light diquark. Since we are considering highly excited heavy baryons, we do not expand the potential of the heavy-quark–light-diquark interaction (6) either in  $p/m_Q$  or in  $p/m_d$  and treat both light diquark and heavy quark fully relativistically. To simplify the potential and to make it local in configuration space we follow the same procedure, which was used for light quarks in a diquark, and replace in Eqs. (6), (7), (9):

(a) the diquark energies

$$E_d(p) \equiv \sqrt{\mathbf{p}^2 + M_d^2} \rightarrow E_d = \frac{M^2 - m_Q^2 + M_d^2}{2M},$$

(b) the heavy quark energies

$$\epsilon_Q(p) \equiv \sqrt{\mathbf{p}^2 + m_Q^2} \rightarrow E_Q = \frac{M^2 - M_d^2 + m_Q^2}{2M}.$$

These substitutions make the Fourier transform of the potential (6) local, but introduce a complicated nonlinear dependence of the potential on the baryon mass  $M$  through the on-mass-shell energies  $E_d$  and  $E_Q$ .

The resulting  $Q\bar{d}$  potential then reads

$$V(r) = V_{\text{SI}}(r) + V_{\text{SD}}(r), \quad (18)$$

where the spin-independent  $V_{\text{SI}}(r)$  part is given by

$$\begin{aligned} V_{\text{SI}}(r) = & \hat{V}_{\text{Coul}}(r) + V_{\text{conf}}(r) + \frac{1}{E_d E_Q} \left\{ \frac{1}{2} (E_Q^2 - m_Q^2 + E_d^2 - M_d^2) [\hat{V}_{\text{Coul}}(r) + V_{\text{conf}}^V(r)] \right. \\ & + \frac{1}{4} \Delta [2V_{\text{Coul}}(r) + V_{\text{conf}}^V(r)] + \hat{V}'_{\text{Coul}}(r) \frac{\mathbf{L}^2}{2r} \left. \right\} + \frac{1}{E_Q (E_Q + m_Q)} \left\{ -(E_Q^2 - m_Q^2) V_{\text{conf}}^S(r) \right. \\ & \left. + \frac{1}{4} \Delta \left( \hat{V}_{\text{Coul}}(r) - V_{\text{conf}}(r) - 2 \left[ \frac{E_Q - m_Q}{2m_Q} - (1 + \kappa) \frac{E_Q + m_Q}{2m_Q} \right] V_{\text{conf}}^V(r) \right) \right\}. \quad (19) \end{aligned}$$

Here  $\Delta$  is the Laplace operator, and  $\hat{V}_{\text{Coul}}(r)$  is the smeared Coulomb potential which accounts for the diquark internal structure

$$\hat{V}_{\text{Coul}}(r) = -\frac{4}{3} \alpha_s \frac{F(r)}{r}.$$

The structure of the spin-dependent potential is given by

$$V_{\text{SD}}(r) = a_1 \mathbf{L} \mathbf{S}_d + a_2 \mathbf{L} \mathbf{S}_Q + b \left[ -\mathbf{S}_d \mathbf{S}_Q + \frac{3}{r^2} (\mathbf{S}_d \mathbf{r})(\mathbf{S}_Q \mathbf{r}) \right] + c \mathbf{S}_d \mathbf{S}_Q, \quad (20)$$

where  $\mathbf{L}$  is the orbital angular momentum;  $\mathbf{S}_d$  and  $\mathbf{S}_Q$  are the diquark and quark spin operators, respectively. The coefficients  $a_1$ ,  $a_2$ ,  $b$  and  $c$  are expressed through the corresponding derivatives of the smeared Coulomb and confining potentials:

$$\begin{aligned} a_1 = & \frac{1}{M_d (E_d + M_d)} \frac{1}{r} \left[ \frac{M_d}{E_d} \hat{V}'_{\text{Coul}}(r) - V'_{\text{conf}}(r) + \mu_d \frac{E_d + M_d}{2M_d} V'_{\text{conf}}{}^V(r) \right] \\ & + \frac{1}{E_d E_Q} \frac{1}{r} \left[ \left( \hat{V}'_{\text{Coul}}(r) + \frac{\mu_d}{2} \frac{E_d}{M_d} V'_{\text{conf}}{}^V(r) \right) + \frac{E_d}{M_d} \left( \frac{E_d - M_d}{E_Q + m_Q} + \frac{E_Q - m_Q}{E_d + M_d} \right) V'_{\text{conf}}{}^S(r) \right], \quad (21) \end{aligned}$$

$$\begin{aligned} a_2 = & \frac{1}{E_d E_Q} \frac{1}{r} \left\{ \hat{V}'_{\text{Coul}}(r) - \left[ \frac{E_Q - m_Q}{2m_Q} - (1 + \kappa) \frac{E_Q + m_Q}{2m_Q} \right] V'_{\text{conf}}{}^V(r) \right\} \\ & + \frac{1}{E_Q (E_Q + m_Q)} \frac{1}{r} \left\{ \hat{V}'_{\text{Coul}}(r) - V'_{\text{conf}}(r) - 2 \left[ \frac{E_Q - m_Q}{2m_Q} - (1 + \kappa) \frac{E_Q + m_Q}{2m_Q} \right] V'_{\text{conf}}{}^V(r) \right\}, \quad (22) \end{aligned}$$

$$\begin{aligned} b = & \frac{1}{3} \frac{1}{E_d E_Q} \left\{ \frac{1}{r} \hat{V}'_{\text{Coul}}(r) - \hat{V}''_{\text{Coul}}(r) \right. \\ & \left. - \frac{\mu_d}{2} \frac{E_d}{M_d} \left[ \frac{E_Q - m_Q}{2m_Q} - (1 + \kappa) \frac{E_Q + m_Q}{2m_Q} \right] \left[ \frac{1}{r} V'_{\text{conf}}{}^V(r) - V''_{\text{conf}}{}^V(r) \right] \right\}, \quad (23) \end{aligned}$$

$$c = \frac{2}{3} \frac{1}{E_d E_Q} \left\{ \Delta \hat{V}_{\text{Coul}}(r) - \frac{\mu_d}{2} \frac{E_d}{M_d} \left[ \frac{E_Q - m_Q}{2m_Q} - (1 + \kappa) \frac{E_Q + m_Q}{2m_Q} \right] \Delta V_{\text{conf}}^V(r) \right\}. \quad (24)$$

Both the one-gluon exchange and confining potential contribute to the quark-diquark spin-orbit interaction. The quasipotential (18)–(24) generalizes the one obtained previously in the framework of the heavy quark  $1/m_Q$  expansion [13]. Note that the expansion of the extended potential (18)–(24) up to the second order in  $1/m_Q$  and the subsequent substitution of the quark energies  $\epsilon_Q(p)$  by the corresponding energies on mass shell  $E_Q$ , reproduces the potential of Ref. [13].

For the scalar diquark ( $S_d = 0$ ) only the term (22), responsible for the heavy quark spin-orbit interaction, contributes to the spin-dependent potential (20), whereas for the axial-vector diquark ( $S_d = 1$ ) all terms (21)–(24) contribute to the spin-dependent potential (20). Solving numerically Eq. (1) with the complete relativistic quasipotential (18) we get the baryon wave function  $\Psi_B$ . Then the total baryon wave function is a product of  $\Psi_B$  and the spin function  $U_B$  (for details see Eq. (43) of Ref. [33]).

It is necessary to note that the presence of the spin-orbit interaction  $\mathbf{L}\mathbf{S}_Q$  and of the tensor interaction in the quark-diquark potential (21)–(23) results in a mixing of states which have the same total angular momentum  $J$  and parity  $P$  but different light diquark total angular momentum ( $\mathbf{L} + \mathbf{S}_d$ ). Such mixing is considered along the same lines as in our previous calculations of the mass spectra of doubly heavy baryons [24].

### III. RESULTS AND DISCUSSION

#### A. Heavy baryon masses

We solve numerically the quasipotential equation with the quasipotential (18) which nonperturbatively accounts for the relativistic dynamics both of the light diquark  $d$  and heavy quark  $Q$ . The calculated values of the ground and excited state baryon masses are given in Tables II–VI in comparison with available experimental data [1]. In the first two columns we give the baryon quantum numbers ( $I(J^P)$ ) and the state of the heavy-quark–light-diquark ( $Qd$ ) bound system (in usual notations  $(n_r + 1)L$ ), while in the remaining columns our predictions for the masses and experimental data are shown.

It is important to note that in the adopted quark-diquark picture of heavy baryons we consider solely the orbital and radial excitations between the heavy quark and light diquark, while light diquarks are taken in the ground (scalar or axial-vector) state. As a result, we get significantly less excited states than in the genuine three-quark picture of a baryon. As it is seen from Tables II–VI, such an approach is supported by available experimental data, which are nicely accommodated in the quark-diquark picture.

Comparing the new values of heavy baryon masses presented in Tables II–VI with the previous results, obtained by using the heavy quark expansion [13], we can estimate the importance of higher order corrections in  $1/m_Q$ . Such comparison confirms expectations that they are mainly important for highly excited heavy baryon states and that charmed baryons are stronger affected than the bottom ones. Indeed, the difference of masses, obtained with and without expansion in  $1/m_Q$ , does not exceed a few MeV for the ground state heavy baryons, while for excited states such difference in some cases reaches tens MeV, especially for the charmed baryons.



TABLE II: Masses of the  $\Lambda_Q$  ( $Q = c, b$ ) heavy baryons (in MeV).

$I(J^P)$	$Qd$ state	$Q = c$		$Q = b$	
		$M$	$M^{\text{exp}} [1]$	$M$	$M^{\text{exp}} [1]$
$0(\frac{1}{2}^+)$	$1S$	2286	2286.46(14)	5620	5620.2(1.6)
$0(\frac{1}{2}^+)$	$2S$	2769	2766.6(2.4)?	6089	
$0(\frac{1}{2}^+)$	$3S$	3130		6455	
$0(\frac{1}{2}^+)$	$4S$	3437		6756	
$0(\frac{1}{2}^+)$	$5S$	3715		7015	
$0(\frac{1}{2}^+)$	$6S$	3973		7256	
$0(\frac{1}{2}^-)$	$1P$	2598	2595.4(6)	5930	
$0(\frac{1}{2}^-)$	$2P$	2983	2939.3( $\frac{1.4}{1.5}$ )?	6326	
$0(\frac{1}{2}^-)$	$3P$	3303		6645	
$0(\frac{1}{2}^-)$	$4P$	3588		6917	
$0(\frac{1}{2}^-)$	$5P$	3852		7157	
$0(\frac{3}{2}^-)$	$1P$	2627	2628.1(6)	5942	
$0(\frac{3}{2}^-)$	$2P$	3005		6333	
$0(\frac{3}{2}^-)$	$3P$	3322		6651	
$0(\frac{3}{2}^-)$	$4P$	3606		6922	
$0(\frac{3}{2}^-)$	$5P$	3869		7171	
$0(\frac{3}{2}^+)$	$1D$	2874		6190	
$0(\frac{3}{2}^+)$	$2D$	3189		6526	
$0(\frac{3}{2}^+)$	$3D$	3480		6811	
$0(\frac{3}{2}^+)$	$4D$	3747		7060	
$0(\frac{5}{2}^+)$	$1D$	2880	2881.53(35)	6196	
$0(\frac{5}{2}^+)$	$2D$	3209		6531	
$0(\frac{5}{2}^+)$	$3D$	3500		6814	
$0(\frac{5}{2}^+)$	$4D$	3767		7063	
$0(\frac{5}{2}^-)$	$1F$	3097		6408	
$0(\frac{5}{2}^-)$	$2F$	3375		6705	
$0(\frac{5}{2}^-)$	$3F$	3646		6964	
$0(\frac{5}{2}^-)$	$4F$	3900		7196	
$0(\frac{7}{2}^-)$	$1F$	3078		6411	
$0(\frac{7}{2}^-)$	$2F$	3393		6708	
$0(\frac{7}{2}^-)$	$3F$	3667		6966	
$0(\frac{7}{2}^-)$	$4F$	3922		7197	
$0(\frac{7}{2}^+)$	$1G$	3270		6598	
$0(\frac{7}{2}^+)$	$2G$	3546		6867	
$0(\frac{9}{2}^+)$	$1G$	3284		6599	
$0(\frac{9}{2}^+)$	$2G$	3564		6868	
$0(\frac{9}{2}^-)$	$1H$	3444		6767	
$0(\frac{11}{2}^-)$	$1H$	3460		6766	

TABLE III: Masses of the  $\Sigma_Q$  ( $Q = c, b$ ) heavy baryons (in MeV).

$I(J^P)$	$Qd$ state	$Q = c$		$Q = b$	
		$M$	$M^{\text{exp}}$ [1]	$M$	$M^{\text{exp}}$ [1]
$1(\frac{1}{2}^+)$	$1S$	2443	2453.76(18)	5808	5807.8(2.7)
$1(\frac{1}{2}^+)$	$2S$	2901		6213	
$1(\frac{1}{2}^+)$	$3S$	3271		6575	
$1(\frac{1}{2}^+)$	$4S$	3581		6869	
$1(\frac{1}{2}^+)$	$5S$	3861		7124	
$1(\frac{3}{2}^+)$	$1S$	2519	2518.0(5)	5834	5829.0(3.4)
$1(\frac{3}{2}^+)$	$2S$	2936	$2939.3(\frac{1.4}{1.5})?$	6226	
$1(\frac{3}{2}^+)$	$3S$	3293		6583	
$1(\frac{3}{2}^+)$	$4S$	3598		6876	
$1(\frac{3}{2}^+)$	$5S$	3873		7129	
$1(\frac{1}{2}^-)$	$1P$	2799	$2802(\frac{4}{7})$	6101	
$1(\frac{1}{2}^-)$	$2P$	3172		6440	
$1(\frac{1}{2}^-)$	$3P$	3488		6756	
$1(\frac{1}{2}^-)$	$4P$	3770		7024	
$1(\frac{1}{2}^-)$	$1P$	2713		6095	
$1(\frac{1}{2}^-)$	$2P$	3125		6430	
$1(\frac{1}{2}^-)$	$3P$	3455		6742	
$1(\frac{1}{2}^-)$	$4P$	3743		7008	
$1(\frac{3}{2}^-)$	$1P$	2798	$2802(\frac{4}{7})$	6096	
$1(\frac{3}{2}^-)$	$2P$	3172		6430	
$1(\frac{3}{2}^-)$	$3P$	3486		6742	
$1(\frac{3}{2}^-)$	$4P$	3768		7009	
$1(\frac{3}{2}^-)$	$1P$	2773	$2766.6(2.4)?$	6087	
$1(\frac{3}{2}^-)$	$2P$	3151		6423	
$1(\frac{3}{2}^-)$	$3P$	3469		6736	
$1(\frac{3}{2}^-)$	$4P$	3753		7003	
$1(\frac{1}{2}^-)$	$1P$	2789		6084	
$1(\frac{1}{2}^-)$	$2P$	3161		6421	
$1(\frac{1}{2}^-)$	$3P$	3475		6732	
$1(\frac{1}{2}^-)$	$4P$	3757		6999	
$1(\frac{3}{2}^+)$	$1D$	3041		6311	
$1(\frac{3}{2}^+)$	$2D$	3370		6636	
$1(\frac{3}{2}^+)$	$1D$	3043		6326	
$1(\frac{3}{2}^+)$	$2D$	3366		6647	
$1(\frac{3}{2}^+)$	$1D$	3040		6285	
$1(\frac{3}{2}^+)$	$2D$	3364		6612	
$1(\frac{3}{2}^+)$	$1D$	3038		6284	
$1(\frac{3}{2}^+)$	$2D$	3365		6612	
$1(\frac{3}{2}^+)$	$1D$	3023		6270	
$1(\frac{3}{2}^+)$	$2D$	3349		6598	

TABLE III: (continued)

$I(J^P)$	$Qd$ state	$Q = c$		$Q = b$	
		$M$	$M^{\text{exp}} [1]$	$M$	$M^{\text{exp}} [1]$
$1(\frac{7}{2}^+)$	$1D$	3013		6260	
$1(\frac{7}{2}^+)$	$2D$	3342		6590	
$1(\frac{5}{2}^-)$	$1F$	3288		6550	
$1(\frac{5}{2}^-)$	$1F$	3283		6564	
$1(\frac{5}{2}^-)$	$1F$	3254		6501	
$1(\frac{7}{2}^-)$	$1F$	3253		6500	
$1(\frac{7}{2}^-)$	$1F$	3227		6472	
$1(\frac{5}{2}^-)$	$1F$	3209		6459	
$1(\frac{5}{2}^+)$	$1G$	3495		6749	
$1(\frac{7}{2}^+)$	$1G$	3483		6761	
$1(\frac{7}{2}^+)$	$1G$	3444		6688	
$1(\frac{5}{2}^+)$	$1G$	3442		6687	
$1(\frac{5}{2}^+)$	$1G$	3410		6648	
$1(\frac{11}{2}^+)$	$1G$	3386		6635	

### B. Regge trajectories of heavy baryons

In the presented analysis we calculated masses of both orbitally and radially excited heavy baryons up to rather high excitation numbers ( $L = 5$  and  $n_r = 5$ ). This makes it possible to construct the heavy baryon Regge trajectories both in the  $(J, M^2)$  and in the  $(n_r, M^2)$  planes. We use the following definitions.

(a) The  $(J, M^2)$  Regge trajectory:

$$J = \alpha M^2 + \alpha_0; \quad (25)$$

(b) The  $(n_r, M^2)$  Regge trajectory:

$$n_r = \beta M^2 + \beta_0, \quad (26)$$

where  $\alpha, \beta$  are the slopes and  $\alpha_0, \beta_0$  are intercepts.

In Figs. 1-5 we plot the Regge trajectories in the  $(J, M^2)$  plane for charmed and bottom baryons with natural ( $P = (-1)^{J-1/2}$ ) and unnatural ( $P = (-1)^{J+1/2}$ ) parities [34]. The Regge trajectories in the  $(n_r, M^2)$  plane are presented in Figs. 6-10. The masses calculated in our model are shown by diamonds. Available experimental data are given by dots with error bars and corresponding baryon names. Straight lines were obtained by a  $\chi^2$  fit of the calculated values. The fitted slopes and intercepts of the Regge trajectories are given in Tables VII and VIII. We see that the calculated heavy baryon masses fit nicely to the linear trajectories in both planes. These trajectories are almost parallel and equidistant.

TABLE IV: Masses of the  $\Xi_Q$  ( $Q = c, b$ ) heavy baryons with the scalar diquark (in MeV).

$I(J^P)$	$Qd$ state	$Q = c$		$Q = b$	
		$M$	$M^{\text{exp}} [1]$	$M$	$M^{\text{exp}} [1]$
$\frac{1}{2}(\frac{1}{2}^+)$	1S	2476	2470.88( $\frac{34}{80}$ )	5803	5790.5(2.7)
$\frac{1}{2}(\frac{1}{2}^+)$	2S	2959		6266	
$\frac{1}{2}(\frac{1}{2}^+)$	3S	3323		6601	
$\frac{1}{2}(\frac{1}{2}^+)$	4S	3632		6913	
$\frac{1}{2}(\frac{1}{2}^+)$	5S	3909		7165	
$\frac{1}{2}(\frac{1}{2}^+)$	6S	4166		7415	
$\frac{1}{2}(\frac{1}{2}^-)$	1P	2792	2791.8(3.3)	6120	
$\frac{1}{2}(\frac{1}{2}^-)$	2P	3179		6496	
$\frac{1}{2}(\frac{1}{2}^-)$	3P	3500		6805	
$\frac{1}{2}(\frac{1}{2}^-)$	4P	3785		7068	
$\frac{1}{2}(\frac{1}{2}^-)$	5P	4048		7302	
$\frac{1}{2}(\frac{3}{2}^-)$	1P	2819	2819.6(1.2)	6130	
$\frac{1}{2}(\frac{3}{2}^-)$	2P	3201		6502	
$\frac{1}{2}(\frac{3}{2}^-)$	3P	3519		6810	
$\frac{1}{2}(\frac{3}{2}^-)$	4P	3804		7073	
$\frac{1}{2}(\frac{3}{2}^-)$	5P	4066		7306	
$\frac{1}{2}(\frac{3}{2}^+)$	1D	3059	3054.2(1.3)	6366	
$\frac{1}{2}(\frac{3}{2}^+)$	2D	3388		6690	
$\frac{1}{2}(\frac{3}{2}^+)$	3D	3678		6966	
$\frac{1}{2}(\frac{3}{2}^+)$	4D	3945		7208	
$\frac{1}{2}(\frac{3}{2}^+)$	1D	3076	3079.9(1.4)	6373	
$\frac{1}{2}(\frac{5}{2}^+)$	2D	3407		6696	
$\frac{1}{2}(\frac{5}{2}^+)$	3D	3699		6970	
$\frac{1}{2}(\frac{5}{2}^+)$	4D	3965		7212	
$\frac{1}{2}(\frac{5}{2}^-)$	1F	3278		6577	
$\frac{1}{2}(\frac{5}{2}^-)$	2F	3575		6863	
$\frac{1}{2}(\frac{5}{2}^-)$	3F	3845		7114	
$\frac{1}{2}(\frac{5}{2}^-)$	4F	4098		7339	
$\frac{1}{2}(\frac{7}{2}^-)$	1F	3292		6581	
$\frac{1}{2}(\frac{7}{2}^-)$	2F	3592		6867	
$\frac{1}{2}(\frac{7}{2}^-)$	3F	3865		7117	
$\frac{1}{2}(\frac{7}{2}^-)$	4F	4120		7342	
$\frac{1}{2}(\frac{7}{2}^+)$	1G	3469		6760	
$\frac{1}{2}(\frac{7}{2}^+)$	2G	3745		7020	
$\frac{1}{2}(\frac{9}{2}^+)$	1G	3483		6762	
$\frac{1}{2}(\frac{9}{2}^+)$	2G	3763		7032	
$\frac{1}{2}(\frac{9}{2}^-)$	1H	3643		6933	
$\frac{1}{2}(\frac{11}{2}^-)$	1H	3658		6934	

TABLE V: Masses of the  $\Xi_Q$  ( $Q = c, b$ ) heavy baryons with the axial vector diquark (in MeV).

$I(J^P)$	$Qd$ state	$Q = c$		$Q = b$
		$M$	$M^{\text{exp}} [1]$	$M$
$\frac{1}{2}(\frac{1}{2}^+)$	1S	2579	2577.9(2.9)	5936
$\frac{1}{2}(\frac{3}{2}^+)$	2S	2983	2971.4(3.3)	6329
$\frac{1}{2}(\frac{5}{2}^+)$	3S	3377		6687
$\frac{1}{2}(\frac{7}{2}^+)$	4S	3695		6978
$\frac{1}{2}(\frac{9}{2}^+)$	5S	3978		7229
$\frac{1}{2}(\frac{1}{2}^+)$	1S	2649	2645.9(0.5)	5963
$\frac{1}{2}(\frac{3}{2}^+)$	2S	3026		6342
$\frac{1}{2}(\frac{5}{2}^+)$	3S	3396		6695
$\frac{1}{2}(\frac{7}{2}^+)$	4S	3709		6984
$\frac{1}{2}(\frac{9}{2}^+)$	5S	3989		7234
$\frac{1}{2}(\frac{1}{2}^-)$	1P	2936	2931(6)	6233
$\frac{1}{2}(\frac{3}{2}^-)$	2P	3313		6611
$\frac{1}{2}(\frac{5}{2}^-)$	3P	3630		6915
$\frac{1}{2}(\frac{7}{2}^-)$	4P	3912		7174
$\frac{1}{2}(\frac{1}{2}^-)$	1P	2854		6227
$\frac{1}{2}(\frac{3}{2}^-)$	2P	3267		6604
$\frac{1}{2}(\frac{5}{2}^-)$	3P	3598		6906
$\frac{1}{2}(\frac{7}{2}^-)$	4P	3887		7164
$\frac{1}{2}(\frac{1}{2}^-)$	1P	2935	2931(6)	6234
$\frac{1}{2}(\frac{3}{2}^-)$	2P	3311		6605
$\frac{1}{2}(\frac{5}{2}^-)$	3P	3628		6905
$\frac{1}{2}(\frac{7}{2}^-)$	4P	3911		7163
$\frac{1}{2}(\frac{1}{2}^-)$	1P	2912		6224
$\frac{1}{2}(\frac{3}{2}^-)$	2P	3293		6598
$\frac{1}{2}(\frac{5}{2}^-)$	3P	3613		6900
$\frac{1}{2}(\frac{7}{2}^-)$	4P	3898		7159
$\frac{1}{2}(\frac{1}{2}^-)$	1P	2929	2931(6)	6226
$\frac{1}{2}(\frac{3}{2}^-)$	2P	3303		6596
$\frac{1}{2}(\frac{5}{2}^-)$	3P	3619		6897
$\frac{1}{2}(\frac{7}{2}^-)$	4P	3902		7156
$\frac{1}{2}(\frac{1}{2}^+)$	1D	3163		6447
$\frac{1}{2}(\frac{3}{2}^+)$	2D	3505		6767
$\frac{1}{2}(\frac{5}{2}^+)$	1D	3167		6459
$\frac{1}{2}(\frac{7}{2}^+)$	2D	3506		6775
$\frac{1}{2}(\frac{9}{2}^+)$	1D	3160		6431
$\frac{1}{2}(\frac{11}{2}^+)$	2D	3497		6751
$\frac{1}{2}(\frac{13}{2}^+)$	1D	3166		6432
$\frac{1}{2}(\frac{15}{2}^+)$	2D	3504		6751
$\frac{1}{2}(\frac{17}{2}^+)$	1D	3153		6420
$\frac{1}{2}(\frac{19}{2}^+)$	2D	3493		6740

TABLE V: (continued)

$I(J^P)$	$Qd$ state	$Q = c$		$Q = b$
		$M$	$M^{\text{exp}} [1]$	$M$
$\frac{1}{2}(7^+)$	$1D$	3147	3122.9(1.3)	6414
$\frac{1}{2}(7^+)$	$2D$	3486		6736
$\frac{1}{2}(33^-)$	$1F$	3418		6675
$\frac{1}{2}(55^-)$	$1F$	3408		6686
$\frac{1}{2}(55^-)$	$1F$	3394		6640
$\frac{1}{2}(7^-)$	$1F$	3393		6641
$\frac{1}{2}(7^-)$	$1F$	3373		6619
$\frac{1}{2}(9^-)$	$1F$	3357		6610
$\frac{1}{2}(55^+)$	$1G$	3623		6867
$\frac{1}{2}(7^+)$	$1G$	3608		6876
$\frac{1}{2}(7^+)$	$1G$	3584		6822
$\frac{1}{2}(9^+)$	$1G$	3582		6821
$\frac{1}{2}(9^+)$	$1G$	3558		6792
$\frac{1}{2}(11^+)$	$1G$	3536		6782

TABLE VI: Masses of the  $\Omega_Q$  ( $Q = c, b$ ) heavy baryons (in MeV).

$I(J^P)$	$Qd$ state	$Q = c$		$Q = b$	
		$M$	$M^{\text{exp}} [1]$	$M$	$M^{\text{exp}} [1]$
$0(\frac{1}{2}^+)$	$1S$	2698	2695.2(1.7)	6064	6071(40)
$0(\frac{1}{2}^+)$	$2S$	3088		6450	
$0(\frac{1}{2}^+)$	$3S$	3489		6804	
$0(\frac{1}{2}^+)$	$4S$	3814		7091	
$0(\frac{1}{2}^+)$	$5S$	4102		7338	
$0(\frac{3}{2}^+)$	$1S$	2768	2765.9(2.0)	6088	
$0(\frac{3}{2}^+)$	$2S$	3123		6461	
$0(\frac{3}{2}^+)$	$3S$	3510		6811	
$0(\frac{3}{2}^+)$	$4S$	3830		7096	
$0(\frac{3}{2}^+)$	$5S$	4114		7343	
$0(\frac{1}{2}^-)$	$1P$	3055		6339	
$0(\frac{1}{2}^-)$	$2P$	3435		6710	
$0(\frac{1}{2}^-)$	$3P$	3754		7009	
$0(\frac{1}{2}^-)$	$4P$	4037		7265	
$0(\frac{1}{2}^-)$	$1P$	2966		6330	
$0(\frac{1}{2}^-)$	$2P$	3384		6706	
$0(\frac{1}{2}^-)$	$3P$	3717		7003	
$0(\frac{1}{2}^-)$	$2P$	4009		7257	
$0(\frac{3}{2}^-)$	$1P$	3054		6340	
$0(\frac{3}{2}^-)$	$2P$	3433		6705	
$0(\frac{3}{2}^-)$	$3P$	3752		7002	

TABLE VI: (continued)

$I(J^P)$	$Qd$ state	$Q = c$		$Q = b$	
		$M$	$M^{\text{exp}}$ [1]	$M$	$M^{\text{exp}}$ [1]
$0(\frac{3}{2}^-)$	$4P$	4036		7258	
$0(\frac{3}{2}^-)$	$1P$	3029		6331	
$0(\frac{3}{2}^-)$	$2P$	3415		6699	
$0(\frac{3}{2}^-)$	$3P$	3737		6998	
$0(\frac{3}{2}^-)$	$4P$	4023		7250	
$0(\frac{5}{2}^-)$	$1P$	3051		6334	
$0(\frac{5}{2}^-)$	$2P$	3427		6700	
$0(\frac{5}{2}^-)$	$3P$	3744		6996	
$0(\frac{5}{2}^-)$	$4P$	4028		7251	
$0(\frac{1}{2}^+)$	$1D$	3287		6540	
$0(\frac{1}{2}^+)$	$2D$	3623		6857	
$0(\frac{3}{2}^+)$	$1D$	3298		6549	
$0(\frac{3}{2}^+)$	$2D$	3627		6863	
$0(\frac{3}{2}^+)$	$1D$	3282		6530	
$0(\frac{3}{2}^+)$	$2D$	3613		6846	
$0(\frac{5}{2}^+)$	$1D$	3297		6529	
$0(\frac{5}{2}^+)$	$2D$	3626		6846	
$0(\frac{5}{2}^+)$	$1D$	3286		6520	
$0(\frac{5}{2}^+)$	$2D$	3614		6837	
$0(\frac{7}{2}^+)$	$1D$	3283		6517	
$0(\frac{7}{2}^+)$	$2D$	3611		6834	
$0(\frac{3}{2}^-)$	$1F$	3533		6763	
$0(\frac{5}{2}^-)$	$1F$	3522		6771	
$0(\frac{5}{2}^-)$	$1F$	3515		6737	
$0(\frac{7}{2}^-)$	$1F$	3514		6736	
$0(\frac{7}{2}^-)$	$1F$	3498		6719	
$0(\frac{9}{2}^-)$	$1F$	3485		6713	
$0(\frac{5}{2}^+)$	$1G$	3739		6952	
$0(\frac{7}{2}^+)$	$1G$	3721		6959	
$0(\frac{7}{2}^+)$	$1G$	3707		6916	
$0(\frac{9}{2}^+)$	$1G$	3705		6915	
$0(\frac{9}{2}^+)$	$1G$	3685		6892	
$0(\frac{11}{2}^+)$	$1G$	3665		6884	

The obtained results allow us to determine the possible quantum numbers of the observed heavy baryons and prescribe them to a particular Regge trajectory. In the  $(J, M^2)$  plane there are three trajectories for which three experimental candidates are available (parent trajectories for the  $\Lambda_c(\frac{1}{2}^+)$  in Fig. 1a, for the  $\Xi_c(\frac{1}{2}^+)$  in Fig. 3a and for the  $\Xi_c^*(\frac{3}{2}^+)$  in Fig. 4b) and two trajectories with two experimental candidates (parent trajectories for the  $\Sigma_c(\frac{1}{2}^+)$  in Fig. 2a and for the  $\Xi_c(\frac{1}{2}^-)$  in Fig. 3b). On the other hand, in the  $(n_r, M^2)$  plane there are three trajectories with two experimental candidates (the  $\Lambda_c(\frac{1}{2}^+)$  and the  $\Lambda_c(\frac{1}{2}^-)$ )

TABLE VII: Fitted parameters  $\alpha$ ,  $\alpha_0$  for the slope and intercept of the  $(J, M^2)$  parent and daughter Regge trajectories for heavy baryons with scalar ( $[q', q]$ ) and axial vector ( $\{q', q\}$ ) diquark ( $q = u, d, q' = u, d, s$ ).

Trajectory	$\alpha$ (GeV $^{-2}$ )	$\alpha_0$	$\alpha$ (GeV $^{-2}$ )	$\alpha_0$
$c[u, d]$	$\Lambda_c \left(\frac{1}{2}^+\right)$		$\Lambda_c \left(\frac{1}{2}^-\right)$	
parent	$0.741 \pm 0.024$	$-3.504 \pm 0.205$	$0.782 \pm 0.030$	$-4.874 \pm 0.276$
1 daughter	$0.793 \pm 0.013$	$-5.626 \pm 0.129$	$0.815 \pm 0.009$	$-6.769 \pm 0.099$
2 daughter	$0.821 \pm 0.005$	$-7.556 \pm 0.052$	$0.839 \pm 0.004$	$-8.654 \pm 0.043$
$c\{q, q\}$	$\Sigma_c \left(\frac{1}{2}^+\right)$		$\Sigma_c^* \left(\frac{3}{2}^+\right)$	
parent	$0.679 \pm 0.032$	$-3.670 \pm 0.278$	$0.778 \pm 0.019$	$-3.498 \pm 0.164$
1 daughter	$0.686 \pm 0.016$	$-5.289 \pm 0.158$	$0.785 \pm 0.001$	$-5.264 \pm 0.012$
2 daughter	0.688	-6.865	0.812	-7.303
$c[s, q]$	$\Xi_c \left(\frac{1}{2}^+\right)$		$\Xi_c \left(\frac{1}{2}^-\right)$	
parent	$0.686 \pm 0.025$	$-3.852 \pm 0.240$	$0.728 \pm 0.020$	$-5.249 \pm 0.211$
1 daughter	$0.739 \pm 0.015$	$-6.025 \pm 0.169$	$0.764 \pm 0.012$	$-7.244 \pm 0.142$
2 daughter	$0.769 \pm 0.008$	$-8.006 \pm 0.103$	$0.789 \pm 0.004$	$-9.168 \pm 0.052$
$c\{s, q\}$	$\Xi'_c \left(\frac{1}{2}^+\right)$		$\Xi_c^* \left(\frac{3}{2}^+\right)$	
parent	$0.643 \pm 0.021$	$-3.856 \pm 0.212$	$0.726 \pm 0.019$	$-3.665 \pm 0.191$
1 daughter	$0.603 \pm 0.026$	$-4.888 \pm 0.272$	$0.667 \pm 0.005$	$-4.614 \pm 0.051$
2 daughter	0.606	-6.413	0.708	-6.865
$c\{s, s\}$	$\Omega_c \left(\frac{1}{2}^+\right)$		$\Omega_c^* \left(\frac{3}{2}^+\right)$	
parent	$0.615 \pm 0.023$	$-4.065 \pm 0.023$	$0.690 \pm 0.020$	$-3.858 \pm 0.205$
1 daughter	$0.565 \pm 0.028$	$-4.910 \pm 0.316$	$0.608 \pm 0.012$	$-4.436 \pm 0.133$
2 daughter	0.558	-6.293	0.668	-6.735
$b[u, d]$	$\Lambda_b \left(\frac{1}{2}^+\right)$		$\Lambda_b \left(\frac{1}{2}^-\right)$	
parent	$0.352 \pm 0.017$	$-10.83 \pm 0.65$	$0.376 \pm 0.014$	$-12.82 \pm 0.58$
1 daughter	$0.397 \pm 0.015$	$-14.33 \pm 0.64$	$0.419 \pm 0.010$	$-16.33 \pm 0.45$
2 daughter	$0.438 \pm 0.015$	$-17.82 \pm 0.68$	$0.460 \pm 0.008$	$-19.84 \pm 0.36$
$b\{q, q\}$	$\Sigma_b \left(\frac{1}{2}^+\right)$		$\Sigma_b^* \left(\frac{3}{2}^+\right)$	
parent	$0.368 \pm 0.014$	$-12.03 \pm 0.55$	$0.404 \pm 0.012$	$-12.34 \pm 0.46$
1 daughter	$0.390 \pm 0.016$	$-14.59 \pm 0.67$	$0.428 \pm 0.014$	$-15.12 \pm 0.58$
2 daughter	0.414	-17.42	0.472	-18.95
$b[s, q]$	$\Xi_b \left(\frac{1}{2}^+\right)$		$\Xi_b \left(\frac{1}{2}^-\right)$	
parent	$0.349 \pm 0.019$	$-11.49 \pm 0.80$	$0.381 \pm 0.014$	$-13.88 \pm 0.60$
1 daughter	$0.399 \pm 0.016$	$-15.27 \pm 0.69$	$0.423 \pm 0.011$	$-17.40 \pm 0.49$
2 daughter	$0.440 \pm 0.015$	$-18.87 \pm 0.70$	$0.465 \pm 0.008$	$-21.03 \pm 0.40$
$b\{s, q\}$	$\Xi'_b \left(\frac{1}{2}^+\right)$		$\Xi_b^* \left(\frac{3}{2}^+\right)$	
parent	$0.356 \pm 0.014$	$-12.16 \pm 0.58$	$0.386 \pm 0.014$	$-12.33 \pm 0.57$
1 daughter	$0.360 \pm 0.053$	$-14.01 \pm 2.31$	$0.386 \pm 0.061$	$-14.11 \pm 2.62$
2 daughter	0.346	-14.95	0.364	-14.83
$b\{s, s\}$	$\Omega_b \left(\frac{1}{2}^+\right)$		$\Omega_b^* \left(\frac{3}{2}^+\right)$	
parent	$0.365 \pm 0.013$	$-13.04 \pm 0.58$	$0.389 \pm 0.011$	$-13.02 \pm 0.47$
1 daughter	$0.378 \pm 0.052$	$-15.30 \pm 2.35$	$0.401 \pm 0.062$	$-15.33 \pm 2.74$
2 daughter	0.373	-16.79	0.391	-16.66



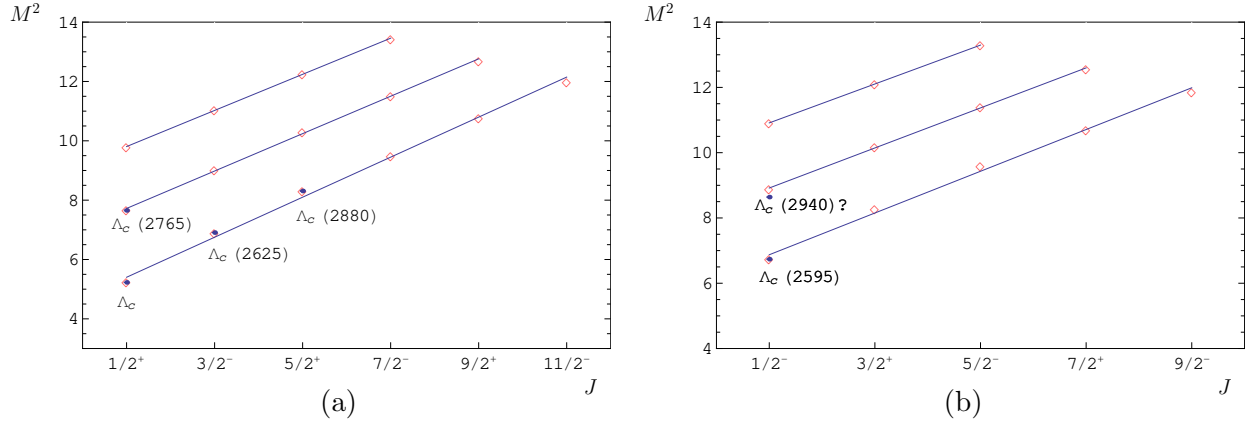


FIG. 1: Parent and daughter  $(J, M^2)$  Regge trajectories for the  $\Lambda_c$  baryons with natural (a) and unnatural (b) parities. Diamonds are predicted masses. Available experimental data are given by dots with particle names;  $M^2$  is in GeV<sup>2</sup>.

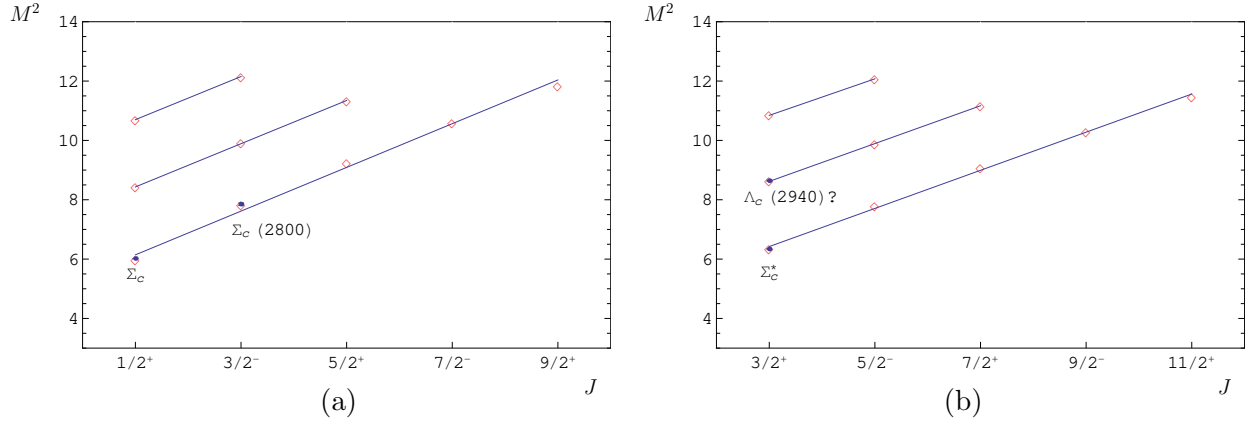


FIG. 2: Same as in Fig. 1 for the  $\Sigma_c$  baryons.

in Fig. 6 and the  $\Xi_c(\frac{1}{2}^+)$  in Fig. 9). All experimental points fit well to the corresponding Regge trajectories obtained in our model.

From Tables II, III and Figs. 1, 2, 6, 7 we see that the  $\Lambda_c(2765)$  (or  $\Sigma_c(2765)$ ),<sup>2</sup> if it is indeed the  $\Lambda_c$  state, can be interpreted in our model as the first radial ( $2S$ ) excitation of the  $\Lambda_c$ . If instead it is the  $\Sigma_c$  state, then it can be identified as its first orbital excitation ( $1P$ ) with  $J = \frac{3}{2}^-$  (see Table III). The  $\Lambda_c(2880)$  baryon corresponds to the second orbital excitation ( $2D$ ) with  $J = \frac{5}{2}^+$ , fitting nicely the parent  $\Lambda_c$  Regge trajectory in the  $(J, M^2)$  plane (see Fig. 1a). Such prescription is in accord with the experimental evidence coming from the  $\Sigma_c(2455)\pi$  decay angular distribution [1]. The other charmed baryon, denoted as

<sup>2</sup> It is important to note that the  $J^P$  quantum numbers for most excited heavy baryons have not been determined experimentally, but are assigned by PDG on the basis of quark model predictions. For some excited charm baryons such as the  $\Lambda_c(2765)$ ,  $\Lambda_c(2880)$  and  $\Lambda_c(2940)$  it is even not known if they are excitations of the  $\Lambda_c$  or  $\Sigma_c$ .

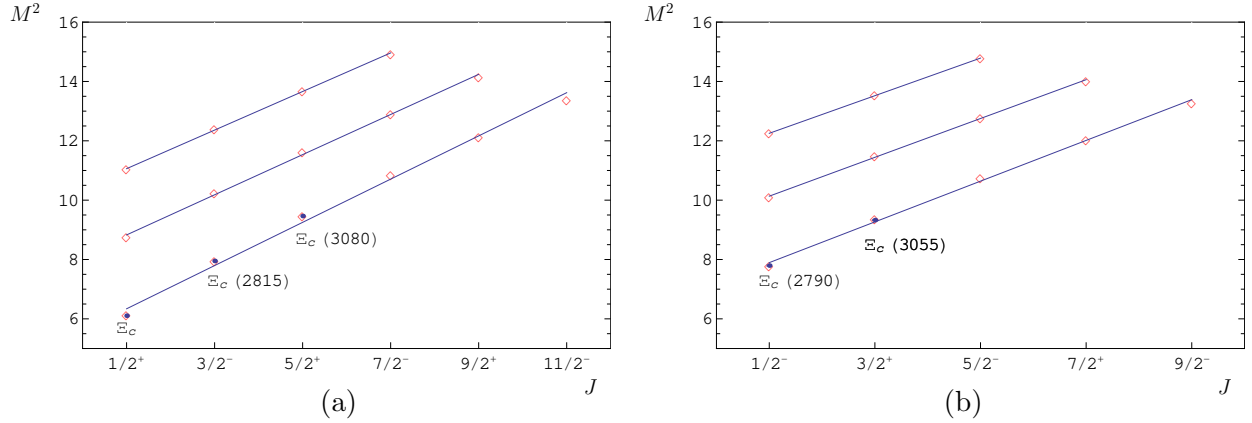


FIG. 3: Same as in Fig. 1 for the  $\Xi_c$  baryons with the scalar diquark.

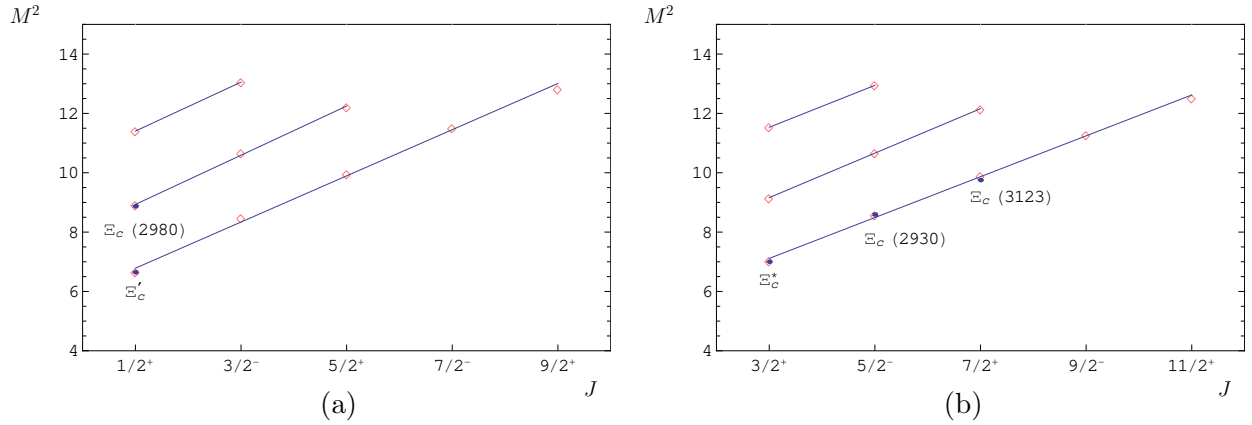
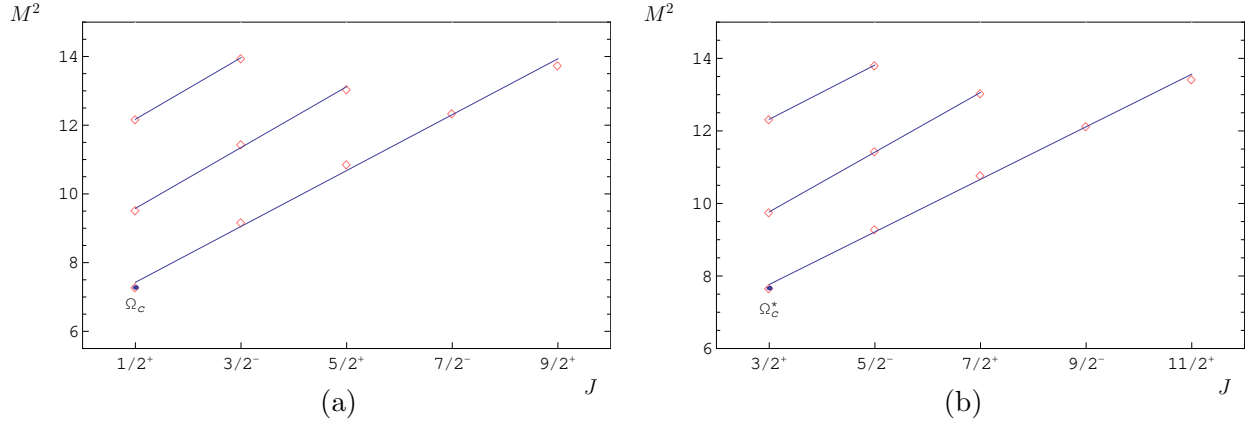
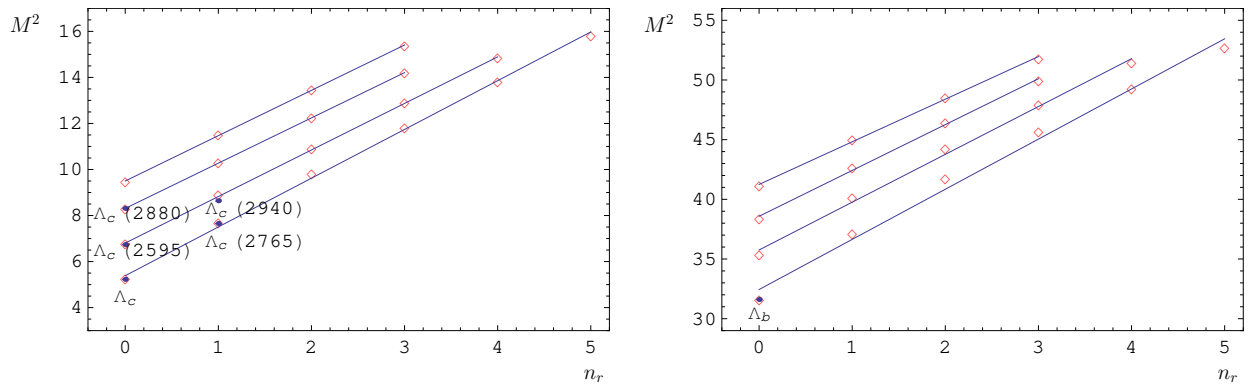


FIG. 4: Same as in Fig. 1 for the  $\Xi'_c$  baryons with the axial vector diquark.

$\Lambda_c(2940)$ , probably has  $I = 0$ , since it was discovered in the  $pD^0$  mass spectrum and not observed in  $pD^+$  channel, but  $I = 1$  is not ruled out [1]. If it is really the  $\Lambda_c$ , state then it could be both an orbitally and radially excited ( $2P$ ) state with  $J = \frac{1}{2}^-$ , whose mass is predicted to be about 40 MeV heavier (see Fig. 1b). A better agreement with experiment (within few MeV) is achieved, if the  $\Lambda_c(2940)$  is interpreted as the first radial excitation ( $2S$ ) of the  $\Sigma_c$  with  $J = \frac{3}{2}^+$  (see Fig. 2b). The  $\Sigma_c(2800)$  can be identified with one of the first orbital ( $1P$ ) excitations of the  $\Sigma_c$  with  $J = \frac{1}{2}^-$  or  $\frac{3}{2}^-$  which have very close masses compatible with experimental value within errors (see Table III).

The results for masses and the Regge trajectories of the  $\Xi_Q$  baryons both with the scalar and axial vector diquarks are given in Tables IV, V and Figs. 3, 4, 8, 9. From these tables and plots we see that the  $\Xi_c(2790)$  and  $\Xi_c(2815)$  can be assigned to the first orbital ( $1P$ ) excitations of the  $\Xi_c$  containing a scalar diquark with  $J = \frac{1}{2}^-$  and  $J = \frac{3}{2}^-$ , respectively. On the other hand, the charmed baryon  $\Xi_c(2930)$  can be considered as either the  $J = \frac{1}{2}^-$ ,  $J = \frac{3}{2}^-$  or  $J = \frac{5}{2}^-$  state (all these states are predicted to have close masses) corresponding to the first orbital ( $1P$ ) excitations of the  $\Xi'_c$  with an axial vector diquark. While the  $\Xi_c(2980)$  can be viewed as the first radial ( $2S$ ) excitation with  $J = \frac{1}{2}^+$  of the  $\Xi'_c$ , the  $\Xi_c(3055)$  and  $\Xi_c(3080)$  baryons can be interpreted as a second orbital ( $2D$ ) excitations of the  $\Xi_c$  containing a scalar

FIG. 5: Same as in Fig. 1 for the  $\Omega_c$  baryons.FIG. 6: The  $(n_r, M^2)$  Regge trajectories for  $\Lambda_Q\left(\frac{1}{2}^+\right)$ ,  $\Lambda_Q\left(\frac{1}{2}^-\right)$ ,  $\Lambda_Q\left(\frac{5}{2}^+\right)$  and  $\Lambda_Q\left(\frac{7}{2}^+\right)$  baryons (from bottom to top). Notations are the same as in Fig. 1.

diquark with  $J = \frac{3}{2}^+$  and  $J = \frac{5}{2}^+$ , and the  $\Xi_c(3123)$  can be viewed as the corresponding  $(2D)$  excitation of the  $\Xi'_c$  with  $J = \frac{7}{2}^+$ .

For the  $\Omega_c$  baryons as well as for all bottom baryons only masses of ground states are known [1], most of which were measured recently. Our original predictions for the ground states [4] of these baryons are very close to the values found in the present analysis (see Tables II-VI) and agree well with measurements [1].

The detailed comparison of our predictions for the masses of the ground and lowest excited states of heavy baryons with the results of other theoretical calculations [5–7] is given in Table 8 of Ref. [13].

### C. Relations between parameters of the Regge trajectories

The slopes of the Regge trajectories, given in Tables VII, VIII, follow in both planes the pattern previously observed for light and heavy mesons [31, 35]. They decrease with the increase of the diquark mass or with the increase of the heavy quark mass. The latter decrease is even more pronounced. The mass dependence of the parameters of the Regge trajectories is the result of the flavour dependence of the potential (18). Such behaviour agrees with the phenomenological consideration of Ref. [23].

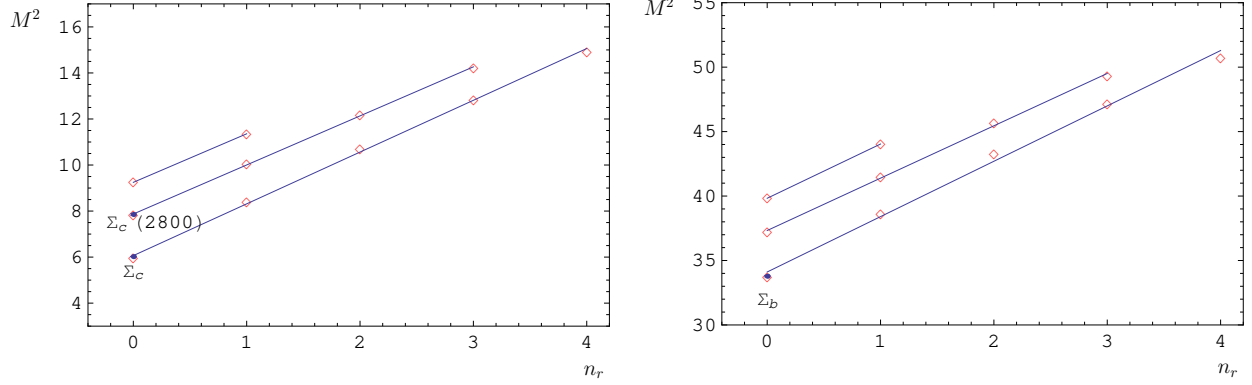


FIG. 7: The  $(n_r, M^2)$  Regge trajectories for  $\Sigma_Q \left(\frac{1}{2}^+, S\right)$ ,  $\Sigma_Q \left(\frac{1}{2}^-, P\right)$  and  $\Sigma_Q \left(\frac{1}{2}^+, D\right)$  baryons (from bottom to top). Notations are the same as in Fig. 1.

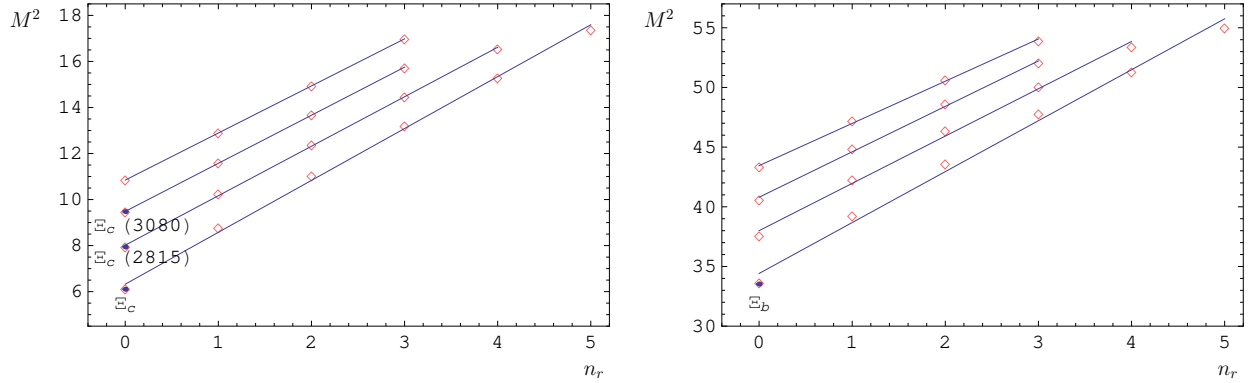


FIG. 8: The  $(n_r, M^2)$  Regge trajectories for  $\Xi_Q \left(\frac{1}{2}^+\right)$ ,  $\Xi_Q \left(\frac{3}{2}^-\right)$ ,  $\Xi_Q \left(\frac{5}{2}^+\right)$  and  $\Xi_Q \left(\frac{7}{2}^-\right)$  baryons (from bottom to top) with the scalar diquark. Notations are the same as in Fig. 1.

It was argued in the literature on the basis of different models within QCD (see e.g. [16, 22, 23] and references therein) that the parameters of the Regge trajectories for the baryon multiplets with given  $J^P$  and different quark constituents can be related by a set of relations, which for heavy baryons is given by:

- (a) the additivity of inverse slopes

$$\frac{1}{\alpha(\Sigma_Q)} + \frac{1}{\alpha(\Omega_Q)} = \frac{2}{\alpha(\Xi'_Q)}, \quad (27)$$

- (b) the additivity of intercepts

$$\alpha_0(\Sigma_Q) + \alpha_0(\Omega_Q) = 2\alpha_0(\Xi'_Q), \quad (28)$$

- (c) the factorization of slopes

$$\alpha(\Sigma_Q)\alpha(\Omega_Q) = \alpha^2(\Xi'_Q). \quad (29)$$

Such relations were extensively used in the literature for obtaining different linear and quadratic mass relations for light and heavy baryons (see e.g. [23] and references therein) and for obtaining on their basis predictions for the baryon masses. However, it was argued

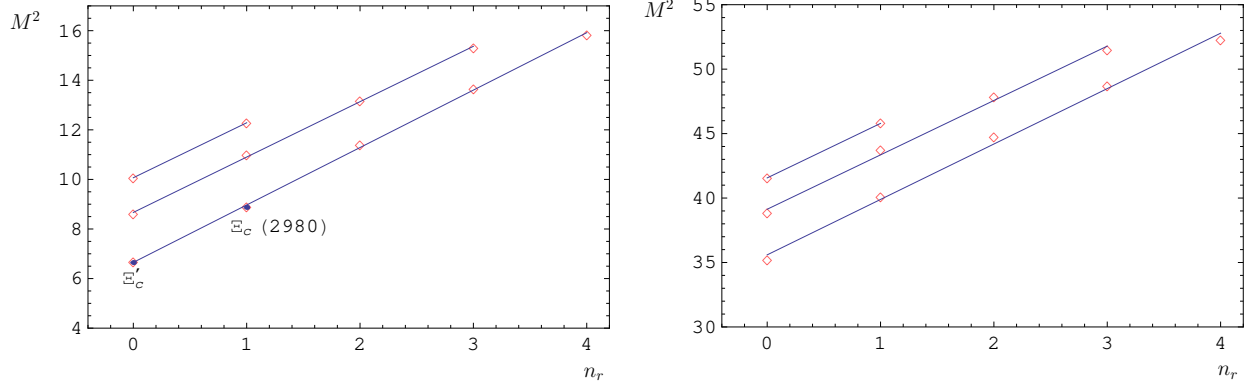


FIG. 9: The  $(n_r, M^2)$  Regge trajectories for  $\Xi'_Q \left(\frac{1}{2}^+\right)$ ,  $\Xi_Q \left(\frac{1}{2}^-\right)$  and  $\Xi_Q \left(\frac{1}{2}^+\right)$  baryons (from bottom to top) with the axial vector diquark. Notations are the same as in Fig. 1.

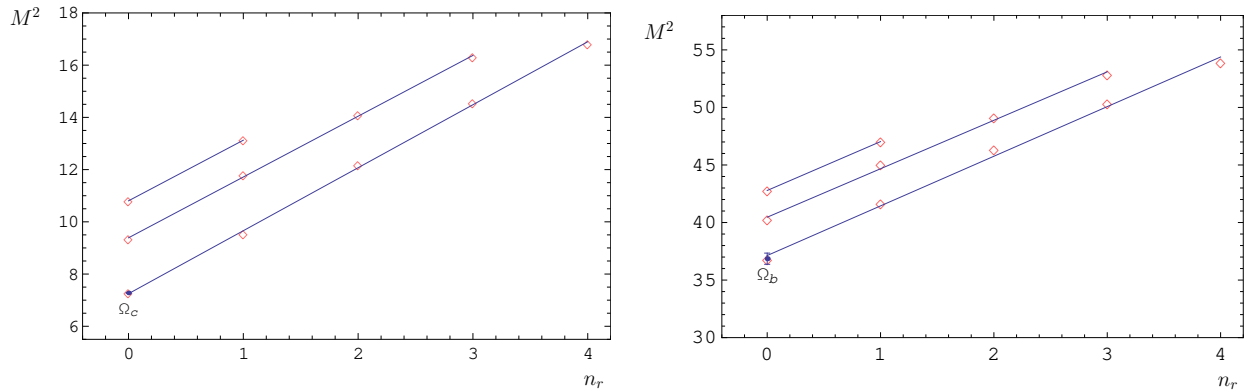


FIG. 10: The  $(n_r, M^2)$  Regge trajectories for  $\Omega_Q \left(\frac{1}{2}^+, S\right)$ ,  $\Omega_Q \left(\frac{1}{2}^-, P\right)$  and  $\Omega_Q \left(\frac{1}{2}^+, D\right)$  baryons (from bottom to top). Notations are the same as in Fig. 1.

in Ref. [16] that relations (27) and (29) are incompatible for heavy baryons. Moreover, it was shown there that the factorization of slopes (29) violates the heavy quark limit for heavy baryons, but this violation introduces rather small errors (less than 15%). The test of the validity of these relations in our model is given in Table IX. It is not surprising that all relations for the slopes are satisfied within the error bars both for parent and daughter trajectories, since the slopes have close values. Let us mention that the slopes of the parent Regge trajectories in the  $(J, M^2)$  plane, obtained in our approach have close values to the ones found in the phenomenological analysis [23], based on the different mass relations for light and heavy baryons.

It is important to compare the values of the slopes of the Regge trajectories for heavy baryons, heavy-light and light mesons. From the comparison of the heavy baryon slopes in Tables VII, VIII we see that the  $\alpha$  values are systematically larger than the  $\beta$  ones. The ratio of their mean values is about 1.5 both for the charmed and bottom baryons. This value of the ratio is very close to the one found for the heavy-light mesons [35] and is slightly larger than the one (1.3) obtained for the light mesons [31].

From comparison of Tables VII, VIII and Tables 4, 5 of Ref. [35] we find that for the same flavour of the heavy quark the heavy baryon slopes have higher values than the heavy-light meson ones. It is interesting that the ratios of the heavy baryon to heavy-light meson slopes

TABLE VIII: Fitted parameters  $\beta$ ,  $\beta_0$  for the slope and intercept of the  $(n_r, M^2)$  Regge trajectories for heavy baryons.

Baryon	$Qd$ state	$Q = c$		$Q = b$	
		$\beta$ (GeV $^{-2}$ )	$\beta_0$	$\beta$ (GeV $^{-2}$ )	$\beta_0$
$\Lambda_Q \left(\frac{1}{2}^+\right)$	$S$	$0.472 \pm 0.010$	$-2.543 \pm 0.099$	$0.238 \pm 0.011$	$-7.722 \pm 0.489$
$\Lambda_Q \left(\frac{1}{2}^-\right)$	$P$	$0.494 \pm 0.006$	$-3.363 \pm 0.059$	$0.248 \pm 0.010$	$-8.848 \pm 0.453$
$\Lambda_Q \left(\frac{3}{2}^-\right)$	$P$	$0.495 \pm 0.005$	$-3.444 \pm 0.053$	$0.249 \pm 0.010$	$-8.925 \pm 0.446$
$\Lambda_Q \left(\frac{5}{2}^+\right)$	$D$	$0.508 \pm 0.003$	$-4.225 \pm 0.030$	$0.260 \pm 0.009$	$-10.05 \pm 0.38$
$\Lambda_Q \left(\frac{7}{2}^-\right)$	$F$	$0.508 \pm 0.005$	$-4.824 \pm 0.059$	$0.280 \pm 0.008$	$-11.55 \pm 0.36$
$\Sigma_Q \left(\frac{1}{2}^+\right)$	$S$	$0.445 \pm 0.009$	$-2.696 \pm 0.089$	$0.233 \pm 0.009$	$-7.942 \pm 0.366$
$\Sigma_Q \left(\frac{1}{2}^-\right)$	$P$	$0.469 \pm 0.006$	$-3.694 \pm 0.070$	$0.246 \pm 0.005$	$-9.190 \pm 0.238$
$\Sigma_Q \left(\frac{5}{2}^-\right)$	$P$	$0.472 \pm 0.006$	$-3.693 \pm 0.069$	$0.249 \pm 0.005$	$-9.256 \pm 0.234$
$\Sigma_Q \left(\frac{1}{2}^+\right)$	$D$	0.474	-4.384	0.238	-9.466
$\Xi_Q \left(\frac{1}{2}^+\right)$	$S$	$0.444 \pm 0.010$	$-2.805 \pm 0.118$	$0.234 \pm 0.010$	$-8.064 \pm 0.464$
$\Xi_Q \left(\frac{1}{2}^-\right)$	$P$	$0.465 \pm 0.007$	$-3.658 \pm 0.078$	$0.251 \pm 0.010$	$-9.527 \pm 0.461$
$\Xi_Q \left(\frac{3}{2}^-\right)$	$P$	$0.465 \pm 0.006$	$-3.729 \pm 0.073$	$0.252 \pm 0.010$	$-9.589 \pm 0.452$
$\Xi_Q \left(\frac{5}{2}^+\right)$	$D$	$0.479 \pm 0.004$	$-4.540 \pm 0.049$	$0.263 \pm 0.009$	$-10.72 \pm 0.40$
$\Xi_Q \left(\frac{7}{2}^-\right)$	$F$	$0.488 \pm 0.001$	$-5.301 \pm 0.017$	$0.282 \pm 0.008$	$-12.28 \pm 0.37$
$\Xi'_Q \left(\frac{1}{2}^+\right)$	$S$	$0.432 \pm 0.006$	$-2.871 \pm 0.060$	$0.233 \pm 0.008$	$-8.279 \pm 0.369$
$\Xi'_Q \left(\frac{1}{2}^-\right)$	$P$	$0.448 \pm 0.007$	$-3.880 \pm 0.087$	$0.237 \pm 0.011$	$-9.276 \pm 0.490$
$\Xi'_Q \left(\frac{5}{2}^-\right)$	$P$	$0.450 \pm 0.007$	$-3.883 \pm 0.078$	$0.240 \pm 0.010$	$-9.379 \pm 0.459$
$\Xi'_Q \left(\frac{1}{2}^+\right)$	$D$	0.451	-4.541	0.236	-9.829
$\Omega_Q \left(\frac{1}{2}^+\right)$	$S$	$0.414 \pm 0.006$	$-3.004 \pm 0.069$	$0.232 \pm 0.008$	$-8.609 \pm 0.385$
$\Omega_Q \left(\frac{1}{2}^-\right)$	$P$	$0.429 \pm 0.008$	$-4.032 \pm 0.098$	$0.237 \pm 0.011$	$-9.608 \pm 0.498$
$\Omega_Q \left(\frac{5}{2}^-\right)$	$P$	$0.432 \pm 0.007$	$-4.049 \pm 0.088$	$0.240 \pm 0.010$	$-9.701 \pm 0.488$
$\Omega_Q \left(\frac{1}{2}^+\right)$	$D$	0.431	-4.654	0.235	-10.07

$(\alpha_{Qqq}/\alpha_{Q\bar{q}}$  and  $\beta_{Qqq}/\beta_{Q\bar{q}}$ ) have very close values, which are about 1.4, both in the  $(J, M^2)$  and in  $(n_r, M^2)$  planes. Note that light baryons and light mesons have almost equal values of the Regge trajectory slopes (see Ref. [2] and references therein).

#### IV. CONCLUSIONS

In this paper the spectroscopy of charmed and bottom baryons was studied in the framework of the quark-diquark picture in the relativistic quark model. The heavy baryon was considered as a heavy-quark-light-diquark bound system in which excitations occur only between a heavy quark and a light diquark. The light diquarks were considered only in the ground (either scalar or axial vector) state. The diquarks were not treated as point-like

TABLE IX: Test of the relations between parameters of the heavy-baryon Regge trajectories in the  $(J, M^2)$  plane.

$J^P$	Traject.	$\frac{1}{\alpha(\Sigma_Q)} + \frac{1}{\alpha(\Omega_Q)}$ (GeV <sup>2</sup> )	$\frac{2}{\alpha(\Xi'_Q)}$ (GeV <sup>2</sup> )	$\alpha_0(\Sigma_Q) + \alpha_0(\Omega_Q)$	$2\alpha_0(\Xi'_Q)$	$\alpha(\Sigma_Q)\alpha(\Omega_Q)$ (GeV <sup>-4</sup> )	$\alpha^2(\Xi'_Q)$ (GeV <sup>-4</sup> )
$Q = c$							
$\frac{1}{2}^+$	parent	$3.10 \pm 0.13$	$3.11 \pm 0.15$	$-7.73 \pm 0.30$	$-7.71 \pm 0.42$	$0.418 \pm 0.035$	$0.414 \pm 0.041$
$\frac{1}{2}^+$	1 daughter	$3.23 \pm 0.12$	$3.32 \pm 0.14$	$-10.20 \pm 0.47$	$-9.78 \pm 0.54$	$0.388 \pm 0.028$	$0.364 \pm 0.031$
$\frac{1}{2}^+$	2 daughter	3.25	3.30	-13.16	-12.83	0.384	0.367
$\frac{3}{2}^+$	parent	$2.74 \pm 0.07$	$2.76 \pm 0.07$	$-7.36 \pm 0.37$	$-7.33 \pm 0.38$	$0.537 \pm 0.029$	$0.527 \pm 0.028$
$\frac{3}{2}^+$	1 daughter	$2.92 \pm 0.04$	$2.99 \pm 0.03$	$-9.70 \pm 0.15$	$-9.23 \pm 0.10$	$0.477 \pm 0.010$	$0.445 \pm 0.009$
$\frac{3}{2}^+$	2 daughter	2.73	2.82	-14.03	-13.73	0.542	0.501
$Q = b$							
$\frac{1}{2}^+$	parent	$5.46 \pm 0.20$	$5.62 \pm 0.22$	$-25.1 \pm 1.1$	$-24.3 \pm 1.2$	$0.134 \pm 0.010$	$0.127 \pm 0.010$
$\frac{1}{2}^+$	1 daughter	$5.26 \pm 0.48$	$5.67 \pm 0.83$	$-29.9 \pm 3.0$	$-28.0 \pm 4.6$	$0.148 \pm 0.026$	$0.132 \pm 0.038$
$\frac{1}{2}^+$	2 daughter	5.10	5.78	-34.2	-29.9	0.154	0.120
$\frac{3}{2}^+$	parent	$5.05 \pm 0.15$	$5.19 \pm 0.19$	$-25.4 \pm 0.9$	$-24.7 \pm 1.1$	$0.157 \pm 0.009$	$0.149 \pm 0.011$
$\frac{3}{2}^+$	1 daughter	$4.89 \pm 0.47$	$5.31 \pm 0.84$	$-30.4 \pm 3.3$	$-28.2 \pm 5.2$	$0.172 \pm 0.032$	$0.153 \pm 0.047$
$\frac{3}{2}^+$	2 daughter	4.68	5.49	-35.6	-29.7	0.184	0.133

objects. Their internal structure was taken into account by including form factors of the diquark-gluon interaction in terms of the diquark wave functions. The dynamics of light quarks inside a diquark as well as the dynamics of a light diquark and a heavy quark inside a baryon were treated completely relativistically without application of either the nonrelativistic  $v/c$  or heavy quark  $1/m_Q$  expansions. Such nonperturbative approach is especially important for the highly excited charmed baryon states, where the heavy quark expansion is not adequate enough. It is important to emphasize that all parameters of our relativistic quark model such as quark masses and parameters of the interquark potential were fixed previously from the investigation of meson mass spectra and decay processes. Thus our model provides a unified universal description of meson and baryon properties.

We calculated the masses of ground, orbitally and radially excited heavy baryons up to rather high excitations ( $L = 5$  and  $n_r = 5$ ). This allowed us to construct the Regge trajectories both in the  $(J, M^2)$  and  $(n_r, M^2)$  planes. It was found that they are almost linear, parallel and equidistant. The available experimental data nicely fit to them. The assignment of the experimentally observed heavy baryons to the particular Regge trajectories was carried out. This allowed us to determine the quantum numbers of the excited heavy baryons. It was found that all currently available experimental data can be well described in the relativistic quark-diquark picture, which predicts significantly less states than the genuine three-body picture.

The comparison of the slopes of the Regge trajectories of heavy baryons and heavy-light mesons was given. It was found that the slope values of heavy baryons are approximately 1.4 times higher than the ones of heavy mesons with the same flavour of the heavy quark.

### Acknowledgments

The authors are grateful to M. Müller-Preussker for support and to V. Matveev, V. Savrin and M. Wagner for discussions. Two of us (R.N.F. and V.O.G.) acknowledge the support by the *Deutsche Forschungsgemeinschaft* under contract Eb 139/6-1.

- 
- [1] K. Nakamura [Particle Data Group], *J. Phys. G* **37**, 075021 (2010).
  - [2] For the recent review see, E. Klempt and J. M. Richard, *Rev. Mod. Phys.* **82**, 1095 (2010).
  - [3] D. Ebert, V. O. Galkin and R. N. Faustov, *Phys. Rev. D* **57**, 5663 (1998); **59**, 019902(E) (1999).
  - [4] D. Ebert, R. N. Faustov and V. O. Galkin, *Phys. Rev. D* **72**, 034026 (2005).
  - [5] S. Capstick and N. Isgur, *Phys. Rev. D* **34**, 2809 (1986).
  - [6] S. Migura, D. Merten, B. Metsch, and H.-R. Petry, *Eur. Phys. J. A* **28**, 41 (2006).
  - [7] H. Garcilazo, J. Vijande and A. Valcarce, *J. Phys. G*, **34**, 961 (2007).
  - [8] J. L. Basdevant and S. Boukraa, *Z. Phys. C* **30**, 103 (1986); R. Roncaglia, D.B. Lichtenberg, and E. Predazzi, *Phys. Rev. D* **52**, 1722 (1995); B. Silvestre-Brac, *Few-Body Systems* **20**, 1 (1996); M. Karliner, B. Keren-Zura, H.J. Lipkin, and J.L. Rosner, arXiv:0706.2163 [hep-ph]; arXiv:0708.4027 [hep-ph]; X. Liu, H.-X. Chen, Y.-R. Liu, A. Hosaka, and S.-L. Zhu, *Phys. Rev. D* **77**, 014031 (2008); W. Roberts and M. Pervin, *Int. J. Mod. Phys. A* **23**, 2817 (2008); A. Valcarce, H. Garcilazo and J. Vijande, *Eur. Phys. J. A* **37**, 217 (2008); I. M. Narodetskii, M. A. Trusov and A. I. Veselov, *Phys. Atom. Nucl.* **72**, 536 (2009); O. N. Driga, I. M. Narodetskii and A. I. Veselov, *Eur. Phys. J. C* **68**, 159 (2010).
  - [9] E. Jenkins, *Phys. Rev. D* **54**, 4515 (1996).
  - [10] R. Lewis and R.M. Woloshyn, *Phys. Rev. D* **79**, 014502 (2009); R. Lewis, arXiv:1010.0889 [hep-lat].
  - [11] M. Wagner and C. Wiese [ETM Collaboration], *PoS LATTICE2010*, 130 (2010) [arXiv:1008.0653 [hep-lat]]; arXiv:1104.4921 [hep-lat].
  - [12] E. Bagan, M. Chabab, H.G. Dosch and S. Narison, *Phys. Lett. B* **278**, 367 (1992); *Phys. Lett. B* **287**, 176 (1992); D.W. Wang, M.Q. Huang, and C.Z. Li, *Phys. Rev. D* **65**, 094036 (2002); Z.G. Wang, *Eur. Phys. J. C* **54**, 231 (2008).
  - [13] D. Ebert, R. N. Faustov and V. O. Galkin, *Phys. Lett. B* **659**, 612 (2008).
  - [14] A. Martin, *Z. Phys. C* **32**, 359 (1986).
  - [15] Yu. A. Simonov, *Phys. Lett. B* **228**, 413 (1989).
  - [16] L. Burakovsky and J. T. Goldman, *Phys. Lett. B* **434**, 251 (1998).
  - [17] A. Inopin and G. S. Sharov, *Phys. Rev. D* **63**, 054023 (2001).
  - [18] A. V. Anisovich, V. V. Anisovich, M. A. Matveev, V. A. Nikonov, A. V. Sarantsev and T. O. Vulfs, *Phys. Atom. Nucl.* **74**, 418 (2011)
  - [19] S. V. Chekanov and B. B. Levchenko, *Phys. Rev. D* **75**, 014007 (2007).
  - [20] H. Forkel, M. Beyer and T. Frederico, *JHEP* **0707**, 077 (2007); H. Forkel and E. Klempt, *Phys. Lett. B* **679**, 77 (2009).
  - [21] S. J. Brodsky and G. F. de Teramond, arXiv:1103.1186 [hep-ph].
  - [22] A. B. Kaidalov, *Z. Phys. C* **12**, 63 (1982).
  - [23] X. H. Guo, K. W. Wei and X. H. Wu, *Phys. Rev. D* **78**, 056005 (2008).
  - [24] D. Ebert, R. N. Faustov, V. O. Galkin and A. P. Martynenko, *Phys. Rev. D* **66**, 014008 (2002).



- [25] D. Ebert, R. N. Faustov and V. O. Galkin, Phys. Lett. B **634**, 214 (2006).
- [26] H. J. Schnitzer, Phys. Rev. D **18**, 3482 (1978).
- [27] D. Ebert, R. N. Faustov and V. O. Galkin, Phys. Rev. D **67**, 014027 (2003).
- [28] R. N. Faustov and V. O. Galkin, Z. Phys. C **66**, 119 (1995).
- [29] A.M. Badalian, A.I. Veselov and B.L.G. Bakker, Phys. Rev. D **70**, 016007 (2004); Yu.A. Simonov, Phys. Atom. Nucl. **58**, 107 (1995).
- [30] D. Shirkov, arXiv:0807.1404 [hep-ph]; D. V. Shirkov and I. L. Solovtsov, Phys. Rev. Lett. **79**, 1209 (1997).
- [31] D. Ebert, R. N. Faustov and V. O. Galkin, Phys. Rev. D **79**, 114029 (2009).
- [32] D. Ebert, R. N. Faustov and V. O. Galkin, Mod. Phys. Lett. A **20**, 1887 (2005); Eur. Phys. J. C **47**, 745 (2006).
- [33] D. Ebert, R. N. Faustov, V. O. Galkin and A. P. Martynenko, Phys. Rev. D **70**, 014018 (2004).
- [34] P. D. B. Collins, "An introduction to Regge theory & high energy physics," Cambridge University Press, Cambridge 1977.
- [35] D. Ebert, R. N. Faustov and V. O. Galkin, Eur. Phys. J. C **66**, 197 (2010).